Adsorbed Intermediates in Oxygen Reduction on Platinum Nanoparticles Observed by In situ IR Spectroscopy

Simantini Nayak,*[a] Ian J. McPherson,[a] and Kylie A. Vincent*[a]

Abstract: The sluggish kinetics of oxygen reduction to water remains a significant limitation in the viability of proton exchange membrane fuel cells, yet details of the four electron oxygen reduction reaction remain elusive. Here we apply in situ infrared spectroscopy to probe surface chemistry of a commercial carbon-supported Pt nanoparticle catalyst during oxygen reduction. Infrared spectra show potential dependent appearance of adsorbed superoxide and hydroperoxide intermediates on Pt. This strongly supports an associative pathway for oxygen reduction. Analysis of the adsorbates alongside the catalytic current suggests that another pathway must also be in operation, consistent with a parallel dissociative pathway.

The oxygen reduction reaction (ORR) in acidic medium is crucial in electrochemistry ranging from corrosion to fuel cell cathodes.[1–5] Over the last five decades, environmentally friendly low-temperature proton exchange membrane fuel cells have faced major performance challenges due to the sluggish kinetics and high overpotential of the ORR, even at Pt nanoparticle cathodes.[6,7] During this time, substantial efforts have been made to find alternatives to expensive Pt catalysts which show similar or better ORR activities.[7–12] However, this effort is hindered by the poor understanding of the ORR mechanism, especially at real supported Pt nanoparticle electrodes. The complete reduction of O_2 to H_2O is a 4-electron process ($O_2 + 4e^- + 4H^+ \rightarrow 2H_2O$) and must therefore be composed of a number of elementary electron transfer steps and intermediate species. Several different mechanistic pathways have been proposed for acidic conditions. One possibility is the initial dissociative adsorption of O_2 to form Pt-O species, which subsequently undergo reduction and protonation. Alternatively the intact O_2 molecule can undergo electron transfer to form superoxide ($O_2 + e^- \rightarrow O_2^{\bullet-}$) and/or (hydro)peroxides ($O_2 + 2e^- + 2H^+ \rightarrow H_2O_2$).[13–17] It is well established from rotating ring disk electrode (RRDE) experiments, which detect species at an outer ring electrode as they diffuse away from a central disk electrode, that the mechanism on Pt proceeds via H_2O_2 as an intermediate.[18–21] Recently, a RRDE was further used to detect solution phase superoxide at a Au ring electrode,[22] while scanning electrochemical microscopy with a nanopipette tip was used to detect desorbed superoxide at the polycrystalline Pt surface during ORR in neutral aqueous solution.[23] However, these electrochemical techniques are not species specific and cannot give any direct structural information or report on ORR intermediates that remain adsorbed on the electrode surface. To get information regarding the adsorbed species at an electrode surface instead of desorbed species, electrochemical techniques must be coupled with surface sensitive spectroscopic methods.

Infrared (IR) spectroscopy, in particular, has proved to be a very powerful experimental technique to study in situ or operando electrocatalytic reactions on metal surfaces,[24–31] including detection of various adsorbed oxygenated species.[32–35] However, so far, most reports of in situ spectroscopic studies have been restricted to thin film metal surfaces, which cannot replicate features of nanoparticle catalysts, such as size dependence.[32,36,37] On the basis of thin Pt film experiments, Adzic and coworkers used a potential-dependent peak at 1005-1016 cm^{-1}, assigned to the O-O stretching mode of adsorbed $O_2^{\bullet-}$ in alkaline ClO_4^- electrolyte, to rule out the dissociative adsorption mechanism,[32] although subsequently ClO_4^- has also been shown to have significant vibrational bands in this spectral region.[35,38] In a different IR study of Pt thin films, this time also with Nafion, Kunimatsu and co-workers report the detection of adsorbed molecular oxygen by the O-O stretch around 1400 cm^{-1}.[34] To date, reports of adsorbed oxygen species are confined to such thin film experiments, although in situ IR spectroscopy was used to study anion adsorption during ORR on a commercial Pt/C catalyst.[38] Details of the ORR mechanism on real, nanoparticle catalysts therefore remain elusive.

Herein we extend our multi-bounce attenuated total reflection infrared (ATR-IR) spectroelectrochemical technique to study adsorbed oxygen intermediates on a commercial carbon supported Pt nanoparticle catalyst (60 wt % Pt/C, HiSPEC 9000, Alfa Aesar) during ORR in acidic 0.1 M $HClO_4$ solution. We use a flow cell we recently reported to ensure effective mass transport during ORR, modified to incorporate a custom-designed diamond-coated silicon internal reflection element (IRE).[31,39] This was essential to avoid spectral interference from the native silicon oxide layer in the 1200-1000 cm^{-1} region. This setup enables in situ observation of adsorbed intermediates on Pt/C as a function of potential during ORR. Details of the electrochemical ATR-IR experiment are presented in Supporting Information.

The ORR mechanism was studied by first cycling the varying the potential (*E*) stepwise from 1.01 V vs SHE down to 0.01 V and back again, in O_2 or Ar-saturated 0.1 M $HClO_4$ solution. The current densities (*j*) are shown in Figure 1a, overlaid on voltammograms also obtained in the ATR-IR cell. The voltammogram under Ar shows features typical of Pt in $HClO_4$. The trace under O_2 reveals a limiting electrocatalytic

[a] Dr. S. Nayak, Dr. I. J. McPherson, Prof. K. A. Vincent
Department of Chemistry
University of Oxford
Inorganic Chemistry Laboratory
South Parks Road, Oxford, OX1 3QR (UK)
E-mail: nayak.me@gmail.com; kylie.vincent@chem.ox.ac.uk

Supporting information for this article is given via a link at the end of the document.

current at potentials below 0.6 V. At each potential step, IR spectra were recorded, with the initial potential 1.01 V acting as the background for the subsequent spectra.

In the spectra recorded under O_2 (Figure 1b) we assign three peaks to oxygen-related species adsorbed on platinum: the band at 1212 ± 3 cm^{-1} we assign to the O-O stretching mode of surface adsorbed superoxide (OOH_{ad}); the band at 1386 ± 4 cm^{-1} we attribute to the OOH bending mode of surface adsorbed hydroperoxide ($HOOH_{ad}$) and the 1468 cm^{-1} band we tentatively assign to the O-O stretching mode of weakly adsorbed molecular oxygen ($O_{2,ad}$). These bands are not observed on the bare carbon support under O_2, but are observed on unsupported Pt nanoparticles (Figure S2a and b in SI).

Isotope substitution experiments were performed by repeating experiments under $^{18}O_2$ and in deuterated electrolyte. The wavenumber position of the 1212 cm^{-1} band undergoes a significant shift to 1164 cm^{-1} under $^{18}O_2$ (Figure S3a in SI), close to the expected value for a pure O-O stretching mode, $1212 \times \sqrt{16/18} = 1142$ cm^{-1}. Its position is unchanged in deuterated medium (Figure S3b in SI), as expected for an O-O mode. A peak at 1169 cm^{-1} was assigned to superoxo-like 2D surface oxides on a Pt(111) surface which was supported by DFT calculations.[40] Pt-O_2 complexes also showed the superoxide O-O stretching mode at 1150 cm^{-1}.[41] On Au(111) the superoxide vibration was calculated to be 1278 cm^{-1}, while on NiOOH peaks were observed between 900-1150 cm^{-1}.[42,43] A peak at 1210 cm^{-1} was assigned to adsorbed superoxide on a Ge surface,[35] while a peak at the slightly higher position of 1250 cm^{-1} was assigned to the same species on Au foil.[44] A peak at 1162 cm^{-1} was assigned to adsorbed superoxide on a rough Bi/Au surface.[45] Interestingly, a peak at 1223 cm^{-1} was observed by Kunimatsu and coworkers at a Nafion coated Pt thin film in an O_2 atmosphere, but was assigned to the strong CF_2 stretching mode from Nafion.[34] No corresponding spectra under inert atmosphere were shown for comparison, but we suggest this peak could have a contribution from an ORR intermediate. We note that in our study we have not used Nafion to avoid such ambiguity.

The 1386 cm^{-1} peak was not detected in the deuterated medium (Figure S3b in SI), presumably because it shifted to low wavenumber beyond the limit of our experimental detection. It showed no shift under $^{18}O_2$ (Figure S3a in SI). These findings are consistent with the 1386 cm^{-1} band arising from the bending mode from a surface-adsorbed hydroperoxide, where the H atom contributes most to the mode and the O atoms remain relatively stationary. The wavenumber position has excellent agreement with the band assigned to hydroperoxide on a Ge surface (1385 cm^{-1})[35] although is higher than the band observed on Au foil (1268 cm^{-1}).[37] Here we note that the O-O stretch of hydroperoxide is normally observed around 815-840 cm^{-1} which is below our detection limit.[46,47]

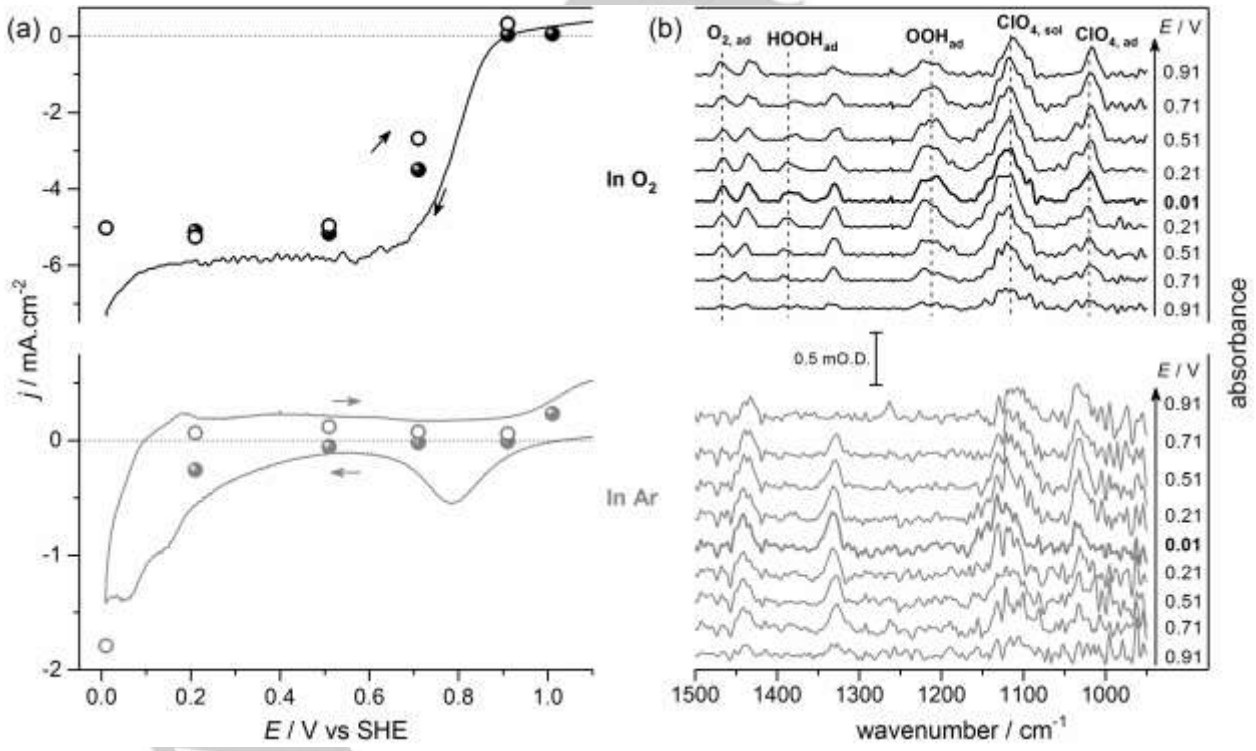

Figure 1. (a) Comparison of voltammetry (lines, scan rate: 2 $mV.s^{-1}$) and average current densities (*j*, closed points: descending potential steps; open points: ascending potential steps) from constant potential application at Pt/C during ORR (black) and under Ar (grey) in 0.1 M $HClO_4$ solution during (b) in situ ATR-IR spectra during constant potential steps shown in (a).

The band at 1468 cm^{-1} appears only in the presence of O_2, and at potentials lower than 0.7 V in the negative-going potential steps, but then remains relatively constant up to 0.9 V during the positive-going potential steps. This band is absent in the $^{18}O_2$ spectrum (Figure S3a in SI). A pure O-O stretching mode at this position would be expected to shift to 1384 cm^{-1} in $^{18}O_2$, but would overlap with the broad peak arising from adsorbed hydroperoxide at 1386 cm^{-1}. We tentatively assign this vibration to the O-O stretch of weakly adsorbed molecular oxygen, $O_{2,ad}$. This assignment agrees with previous reports of adsorbed O_2 where peaks were observed around 1400 cm^{-1} for the Pt/Nafion interface using in situ IR,[34] and at 1550 cm^{-1} on a rough Bi/Au film using SERS.[45]

The IR peaks at 1114 cm^{-1} and 1030 cm^{-1} are not from O_2-derived species as they are observed under Ar, and the 1114 cm^{-1} band is also seen in the absence of Pt, on the bare carbon support. From spectra of the pure $HClO_4$ solution we can attribute the 1114 cm^{-1} peak to the asymmetric ClO_4 stretch of the supporting electrolyte, while we can assign its partner at 1030 cm^{-1} to the symmetric ClO_3 stretching mode of adsorbed $ClO_{4,ads}$ based on previous studies.[35,38,45,47,48] The remaining peaks, at 1435 cm^{-1} and 1330 cm^{-1}, were also present in spectra of the bare carbon support (Figure S2 in SI), and are therefore assigned to carbon surface functionalities.[38] A minor peak at 1260 cm^{-1}, observed occasionally during the potential scan, is assigned to the Si-O-Si band from the silicone glue used to seal the optic.

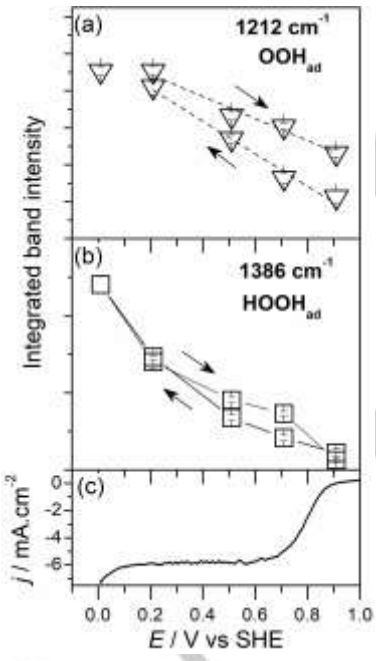

Figure 2. Comparison of band intensities of (a) 1212 cm^{-1} and (b) 1386 cm^{-1} bands during negative- and positive-going potential steps, with the current density (c) measured separately during voltammetry, at Pt/C catalyst in O_2 saturated solutions of 0.1 M $HClO_4$ during in situ ATR-IR experiments. The error bars represent the uncertainty in fitted values based on standard deviations from the Gaussian peak fitting.

ORR on platinum has been proposed to proceed via either associative or dissociative adsorption of O_2, or a combination of these pathways operating in parallel.[16,17,49–51] The in situ observation of OOH_{ad} and $HOOH_{ad}$ during ORR on Pt/C is strongly indicative of an associative pathway in which the O-O bond breaking only occurs at the peroxo level. Figure 2 shows the potential dependence of these adsorbed species obtained from the integrated intensities via peak fitting (see Figure S4 in SI). Adsorbed superoxide, OOH_{ad} is present at potentials as high as 0.9 V, while the adsorbed hydroperoxide, $HOOH_{ad}$ is only observed below the onset potential for ORR. It is striking that the intensities of these intermediates continue to increase during the current plateau region. This would be consistent with the presence of a second, parallel ORR pathway which does not involve the same adsorbed intermediates, and makes a greater contribution at high potential, Scheme 1. This aligns well with Norskov's proposal on the basis of DFT calculations of parallel associative and dissociative pathways, with the associative path dominating at potentials of 0.8 V and below.[16] The origin of this switch in pathways can be understood by considering that at more negative potentials, electronic back donation favours $HOOH_{ad}$ decomposition, while hindering Pt-O bond cleavage, an effect also confirmed by calculations.[52]

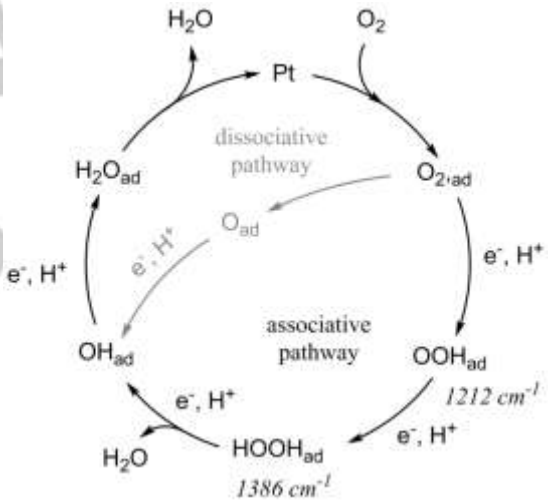

Scheme 1. Proposed mechanism of ORR at Pt/C nanoparticle catalyst in 0.1 M $HClO_4$ solution. The associative pathway makes a greater contribution at lower potentials.

In summary, observation of potential dependent superoxide and hydroperoxide peaks shows that the ORR must involve a contribution from the associative pathway. Our in situ approach further enables correlation of the catalytic current, in both kinetic and diffusion control regimes, with the intensity of adsorbed surface species. Analysis of this data provides evidence for an additional pathway being in operation, consistent with a parallel dissociative route, Scheme 1, with the associative pathway making the greatest contribution at lower potentials. This insight into the complex ORR mechanism at a

commercial nanoparticle catalyst surface will be valuable in the targeted design of improved and more efficient catalysts for this important fuel cell reaction.

Acknowledgements

S.N. acknowledges financial support from the European Union's Horizon 2020 research and innovation programme under the Marie Sklodowska-Curie grant (659306). I.J.M and K.A.V acknowledge support from the European Research Council (ERC, EnergyBioCatalysis-ERC-2010-StG-258600).

Keywords: IR spectroscopy • electrochemistry • oxygen reduction • reaction mechanisms • platinum

[1] M. Stratmann, J. Müller, *Corros. Sci.* **1994**, *36*, 327–359.
[2] M. Shao, Q. Chang, J.-P. Dodelet, R. Chenitz, *Chem. Rev.* **2016**, *116*, 3594–3657.
[3] Y. Nie, L. Li, Z. Wei, *Chem. Soc. Rev.* **2015**, *44*, 2168–2201.
[4] J. Greeley, I. E. L. Stephens, A. S. Bondarenko, T. P. Johansson, H. A. Hansen, T. F. Jaramillo, J. Rossmeisl, I. Chorkendorff, J. K. Nørskov, *Nat. Chem.* **2009**, *1*, 552–556.
[5] N. M. Markovic, P. N. Ross Jr., *Surf. Sci. Rep.* **2002**, *45*, 117–229.
[6] K. J. J. Mayrhofer, M. Arenz, *Nat. Chem.* **2009**, *1*, 518–519.
[7] J. Wu, H. Yang, *Acc. Chem. Res.* **2013**, *46*, 1848–1857.
[8] I. E. L. Stephens, A. S. Bondarenko, U. Grønbjerg, J. Rossmeisl, I. Chorkendorff, *Energy Environ. Sci.* **2012**, *5*, 6744.
[9] N. V. Long, Y. Yang, C. Minh Thi, N. Van Minh, Y. Cao, M. Nogami, *Nano Energy* **2013**, *2*, 636–676.
[10] S. Guo, S. Zhang, S. Sun, *Angew. Chemie - Int. Ed.* **2013**, *52*, 8526–8544.
[11] J. Greeley, I. E. L. Stephens, A. S. Bondarenko, T. P. Johansson, H. A. Hansen, T. F. Jaramillo, J. Rossmeisl, I. Chorkendorff, J. K. Nørskov, *Nat. Chem.* **2009**, *1*, 552–556.
[12] A. A. Gewirth, J. A. Varnell, A. M. Diascro, *Chem. Rev.* **2018**, *118*, 2313–2339.
[13] J. P. Hoare, *The Electrochemistry of Oxygen*, Interscience, New York, **1968**.
[14] K. Kinoshita, *Electrochemical Oxygen Technology*, Wiley, New York, Vol. 1117, **1992**.
[15] N. Ramaswamy, S. Mukerjee, *Adv. Phys. Chem.* **2012**, *2012*, 1–17.
[16] J. K. Nørskov, J. Rossmeisl, A. Logadottir, L. Lindqvist, J. R. Kitchin, T. Bligaard, H. Jónsson, *J. Phys. Chem. B* **2004**, *108*, 17886–17892.
[17] N. A. Anastasijević, V. Vesović, R. R. Adžić, *J. Electroanal. Chem.* **1987**, *229*, 305–316.
[18] N. M. Markovic, H. A. Gasteiger, P. N. Ross, *J. Phys. Chem.* **1995**, *99*, 3411–3415.
[19] L. Geniès, R. Faure, R. Durand, *Electrochim. Acta* **1998**, *44*, 1317–1327.
[20] U. A. Paulus, T. J. Schmidt, H. A. Gasteiger, R. J. Behm, *J. Electroanal. Chem.* **2001**, *495*, 134–145.
[21] L. Zhang, H. Li, J. Zhang, *J. Power Sources* **2014**, *255*, 242–250.
[22] Z. Feng, N. S. Georgescu, D. A. Scherson, *Anal. Chem.* **2016**, *88*, 1088–1091.
[23] M. Zhou, Y. Yu, K. Hu, M. V. Mirkin, *J. Am. Chem. Soc.* **2015**, *137*, 6517–6523.
[24] M. Heinen, Y. X. Chen, Z. Jusys, R. J. Behm, *Electrochim. Acta* **2007**, *52*, 5634–5643.
[25] Y. Y. Yang, J. Ren, Q. X. Li, Z. Y. Zhou, S. G. Sun, W. Bin Cai, *ACS Catal.* **2014**, *4*, 798–803.
[26] J. Y. Wang, H. X. Zhang, K. Jiang, W. Bin Cai, *J. Am. Chem. Soc.* **2011**, *133*, 14876–14879.
[27] Y. X. Chen, S. Ye, M. Heinen, Z. Jusys, M. Osawa, R. J. Behm, *J. Phys. Chem. B* **2006**, *110*, 9534–9544.
[28] C. Keresszegi, D. Ferri, T. Mallat, A. Baiker, *J. Phys. Chem. B* **2004**, *109*, 958–967.
[29] H. Wang, B. Jiang, T. T. Zhao, K. Jiang, Y. Y. Yang, J. Zhang, Z. Xie, W. Bin Cai, *ACS Catal.* **2017**, *7*, 2033–2041.
[30] I. Kendrick, J. Doan, E. S. Smotkin, in *Vib. Spectrosc. Electrified Interfaces*, John Wiley & Sons, Inc., New Jersey, **2013**, pp. 327–344.
[31] I. J. McPherson, P. A. Ash, R. M. J. Jacobs, K. A. Vincent, *Chem. Commun.* **2016**, *52*, 12665–12668.
[32] M. Shao, P. Liu, R. R. Adzic, *J. Am. Chem. Soc.* **2006**, *128*, 7408–7409.
[33] S. Nayak, P. U. Biedermann, M. Stratmann, A. Erbe, *Electrochim. Acta* **2013**, *106*, 472–482.
[34] K. Kunimatsu, T. Yoda, D. A. Tryk, H. Uchida, M. Watanabe, *Phys. Chem. Chem. Phys.* **2010**, *12*, 621–629.
[35] S. Nayak, P. U. Biedermann, M. Stratmann, A. Erbe, *Phys. Chem. Chem. Phys.* **2013**, *15*, 5771–5781.
[36] M. Nesselberger, S. Ashton, J. C. Meier, I. Katsounaros, K. J. J. Mayrhofer, M. Arenz, *J. Am. Chem. Soc.* **2011**, *133*, 17428–17433.
[37] M. H. Shao, R. R. Adzic, *J. Phys. Chem. B* **2005**, *109*, 16563–16566.
[38] M. Nesselberger, M. Arenz, *ChemCatChem* **2016**, *8*, 1125–1131.
[39] R. Hidalgo, P. A. Ash, A. J. Healy, K. A. Vincent, *Angew. Chemie Int. Ed.* **2015**, *54*, 7110–7113.
[40] Y. F. Huang, P. J. Kooyman, M. T. M. Koper, *Nat. Commun.* **2016**, *7*, 1–7.
[41] D. A. Pankratov, V. B. Sokolov, Y. M. Kiselev, *Russ. J. Inorg. Chem.* **2000**, *45*, 1388–1393.
[42] O. Diaz-Morales, F. Calle-Vallejo, C. de Munck, M. T. M. Koper, *Chem. Sci.* **2013**, *4*, 2334–2343.
[43] O. Diaz-Morales, D. Ferrus-Suspedra, M. T. M. Koper, *Chem. Sci.* **2016**, *7*, 2639–2645.
[44] J. Brooker, P. A. Christensen, A. Hamnett, R. He, C. A. Paliteiro, *Faraday Discuss.* **1992**, *94*, 339–360.
[45] X. Li, A. A. Gewirth, *J. Am. Chem. Soc.* **2005**, *127*, 5252–5260.
[46] B. S. Yeo, S. L. Klaus, P. N. Ross, R. A. Mathies, A. T. Bell, *ChemPhysChem* **2010**, *11*, 1854–1857.
[47] X. Li, A. A. Gewirth, *J. Raman Spectrosc.* **2005**, *36*, 715–724.
[48] C. I. Ratcliffe, D. E. Irish, *Can. J. Chem.* **1985**, *63*, 3521–3525.
[49] A. Damjanovic, M. A. Genshaw, J. O'M Bockris, *J. Chem. Phys.* **1966**, *45*, 4057–4059.
[50] H. S. Wroblowa, Y. C. Pan, G. Razumney, *J. Electroanal. Chem. Interfacial Electrochem.* **1976**, *69*, 195–201.
[51] E. Yeager, *Electrochim. Acta* **1984**, *29*, 1527–1537.
[52] A. Panchenko, M. T. M. Koper, T. E. Shubina, S. J. Mitchell, E. Roduner, *J. Electrochem. Soc.* **2004**, *151*, A2016–A2027.

Entry for the Table of Contents

COMMUNICATION

In situ IR spectroscopy provides insight into the mechanism of the oxygen reduction reaction on supported platinum. Observation of adsorbed superoxide and hydroperoxide provides evidence for an associative contribution to the mechanism. Further correlation with the catalytic current suggests an additional pathway is also important at high potential.

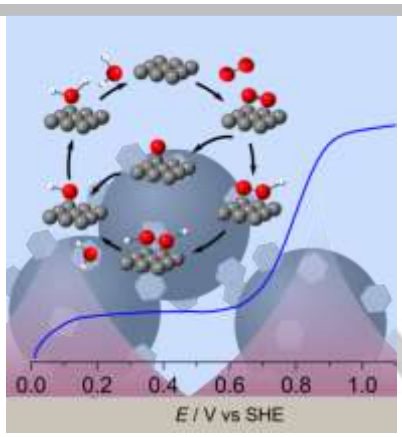

Simantini Nayak, Ian J. McPherson, and Kylie A. Vincent*

Page No. – Page No.
Adsorbed Intermediates in Oxygen Reduction on Platinum Nanoparticles Observed by In situ IR Spectroscopy